COLD-RING SHAPED STORMS IN CENTRAL EUROPE

Martin Setvák[1], Daniel T. Lindsey[2], Petr Novák[1], Robert M. Rabin[3], Pao K. Wang[4], Jochen Kerkmann[5], Michaela Radová[1], Jindřich Šťástka[1]

[1] Czech Hydrometeorological Institute, Na Šabatce 17, CZ-14306 Praha 4, Czech Republic
[2] NOAA/NESDIS/RAMMB, CIRA/CSU, 1375 Campus Delivery, Ft. Collins, CO 80523, U.S.A.
[3] NOAA/National Severe Storms Laboratory, 120 David L. Boren Blvd, Norman, OK 73072, U.S.A.
[4] University of Wisconsin-Madison, 1225 W. Dayton Street, Madison, WI 53706, U.S.A.
[5] EUMETSAT, Am Kavalleriesand 31, D-64295 Darmstadt, Germany

Abstract

This paper addresses satellite observations of Central European convective storms which exhibit a cloud-top feature resembling a cold ring in the IR-window bands, surrounding a distinct central warm spot (CWS). The storms from 25 June 2006 above the Czech Republic and Austria (Figure 1), the prime topic of this paper, are extraordinary examples of storms with such features – not only by the magnitude and duration of the cold ring and CWS couplets, but namely by storm cloud-top heights as determined from radar observations. While the cold-ring shaped storms in general are not rare, their duration is usually much shorter and the magnitude is typically smaller as compared to this case. The paper documents this case on the basis of MSG observations, combined with C-band radar data. Further, it discusses the potential of the satellite-observed cold-ring feature as one of the indicators of storm severity. Finally, the paper briefly notes the possible impacts of this feature on some cloud-top related products derived from satellite imagery, namely the cloud top height.

INTRODUCTION

The *cold-ring shaped storms* belong to a more general category of storms whose tops have distinct cold/warm couplets. Warm spots embedded within the cold anvil tops were first reported some 30 years ago, on the basis of GOES/SMS imagery (Mills and Astling, 1977). In the 1980's the topic received more attention when a special category of storms, called *enhanced-V shaped storms*, was documented in detail, e.g. by Negri (1982), Fujita (1982), McCann (1983), and Heymsfield (1983a). The original name of this feature reflects the fact that it was revealed in *enhanced IR imagery*; however presently we prefer to use a more physically accurate and descriptive term for this feature, *cold-U* (or cold-V, sometimes also cold-U/V) shape. Follow-up works, e.g. of Heymsfield et al. (1983b), Schlesinger (1984, 1988), Adler et al. (1985), Adler and Mack (1986), Heymsfield and Blackmer (1988), and Heymsfield et al. (1991) discussed the origins of this feature and namely of the warm regions enclosed by this feature – *close-in warm area*, CWA, and *distant warm area*, DWA. They also documented a close link between the occurrence and magnitude of these features, and the storm severity. An example of a cold-U shaped storm as observed by MSG satellite is shown in Figure 1. Recently, the topic has again increased in importance in relation to gravity wave breaking, e.g. Wang (2007), *pyro-Cb* storms, e.g. Luderer et al. (2007), or possible nowcasting utilization, e.g. Brunner et al. (2007). We mention this type of storm here because there appears to be a very close link between the cold-U/V shaped storms and storms with the *cold-ring* feature atop their anvils. Therefore, the studies above should be considered carefully when discussing cold-ring shaped storms.

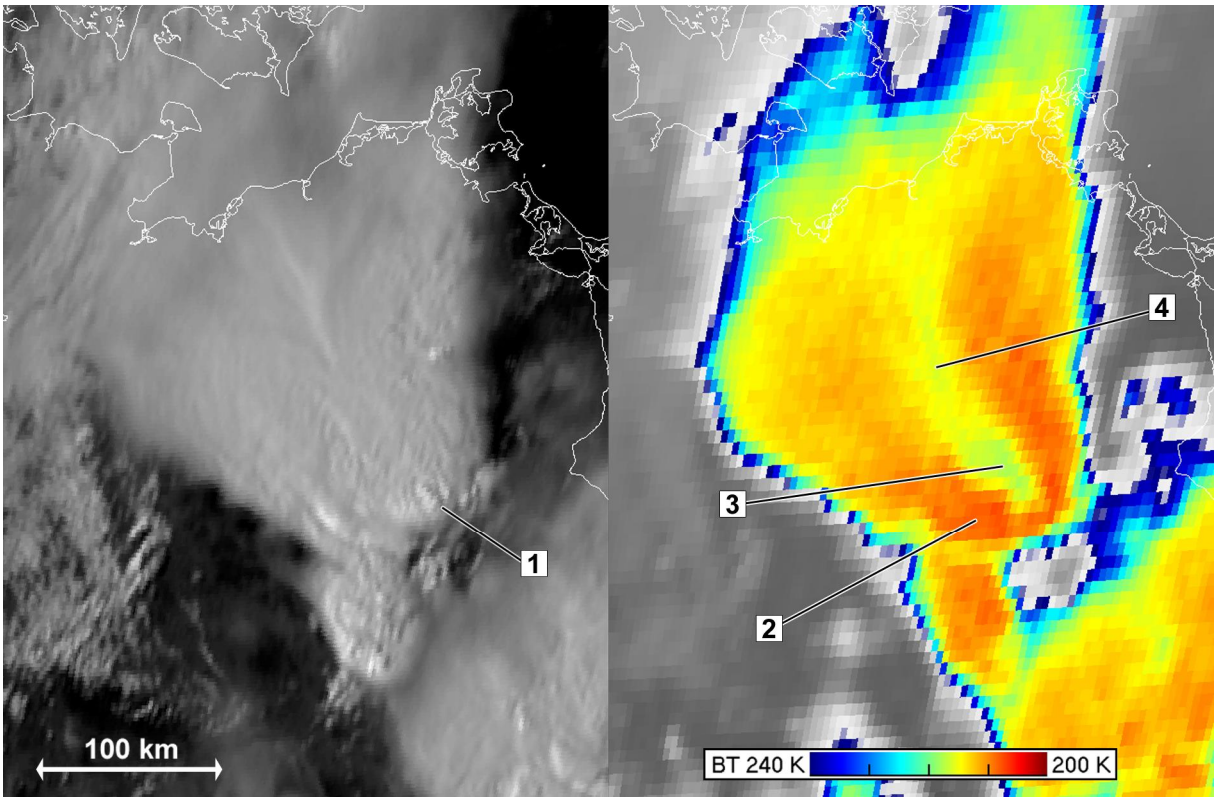

Figure 1: **Example of a cold-U shaped storm. 26 May 2007 15:10 UTC, Meteosat-9 (MSG-2), NE Germany. HRV image left, color enhanced IR10.8 image right (temperature scale bar inserted). Legend: 1 - overshooting tops, 2 - cold-U shape, 3 - close-in warm area (CWA), 4 - distant warm area (DWA).**

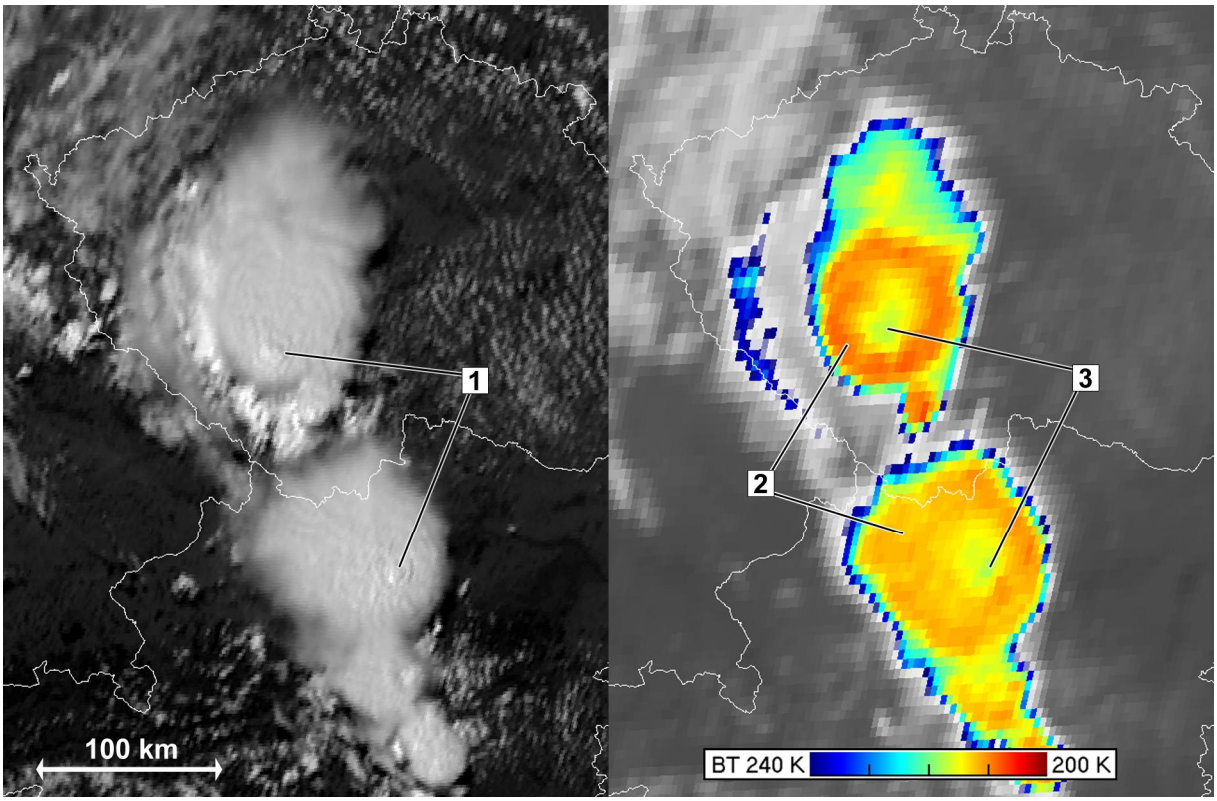

Figure 2: **Example of cold-ring shaped storms. 25 June 2006 13:55 UTC, Meteosat-8 (MSG-1), Czech Republic and Austria. HRV image left, color enhanced IR10.8 image right (temperature scale bar inserted). Legend: 1 - overshooting tops, 2 - cold ring, 3 - central warm spot (CWS).**

C*old-ring shaped storms* are similar to those having cold-U shapes, with the main distinction being the closed shape of the cold feature (Figure 2). The cold ring entirely encloses the *central warm spot* (CWS). Despite the high probability that the origin of the CWS is similar to the origin of the CWA inside cold-U shaped storms (and therefore both warm features might be named the same), for practical reasons we prefer to distinguish the two features by different names. If the origin of both (CWA and CWS) proves to be the same, it is likely that the terminology will be unified in the future.

Though several cases of cold-ring shaped storms have been known earlier (either unpublished, or documented e.g. by Dotzek et al, 2005), it was the launch of MSG satellite with its SEVIRI imager which started a period of their more frequent observations over Europe. Whether it was a result of the higher geometrical resolution of the SEVIRI instrument in combination with a better spectral response of the MSG sensors at the lowest temperatures, or just a coincidence of some other factors remains uncertain. This paper addresses the central-European storms (namely the case from 25 June 2006, Fig.2); however, similar cold-ring shaped storms have also been observed elsewhere over Europe, as well as in other geographical regions. This paper also summarizes some of the observational characteristics of the cold-ring and central warm spot (CWS) features, discussing their possible operational impacts. A more detailed formal paper will follow, addressing also some other aspects related to these types of storms and their link to those having cold-U shapes.

STORMS OF 25 JUNE 2006 ABOVE THE CZECH REPUBLIC AND AUSTRIA

The storms which occurred above the Czech Republic and Austria on 25 June 2006 represent some of the best examples of cold-ring shaped storms. The evolution of these storms in the enhanced IR10.8 imagery is shown in Figure 3, and their appearance in radar data in Figure 4. From the radar side-views of the operational maximum reflectivity product (Fig. 4 top) it is obvious that the storms have extended well above the upper limit of this product (14 km Novak, 2007), and therefore the raw radar data were reprocessed up to the 20 km level. A cross-section based on this operational product is shown at the bottom of Fig. 4, documenting that the tops of these storms have reached 18 - 20 km. Even if we consider all the possible errors and uncertainties of this radar product, it is obvious that these storms were exceptional not only by their satellite appearance, but also by their heights.

For any inferences on the origin of the cold ring and CWS, it is crucial to know as precisely as possible the location of the highest overshooting tops (or in this case a “dome”) with respect to the satellite-observed features. Already the comparison of visible imagery (HRV band) with the enhanced IR10.8 (e.g. Fig. 2) shows that the overshooting tops are located at the southernmost part of the cold ring, partially extending into the CWS. This has been validated by comparing the radar and MSG data, after applying parallax correction (Radová and Seidl, 2008). Taking into account the significant penetration of the highest storm tops into the warmer lower stratosphere, it was likely that the satellite-derived cloud top products may fail in this case, and therefore a different approach was applied. The individual radar CAPPI (derived radar reflectivity at constant altitude) levels up to 20 km were shifted using the parallax correction, as if observed from MSG satellite, and then compared to the MSG data (Figures 5 and 6). This method has shown that the highest tops are located at the upwind side of the cold ring, and that the CWS develops with time downwind of these. Fig. 7 shows the evolution of the storms above south Czech Republic in radar cross-sections, with the position of the CWS indicated by double-arrows. The timing of satellite and radar observations has posed a certain “coherence” problem when comparing the two datasets (MSG data available every 15 minutes, radar data every 10 minutes), which is the reason why the position of CWS in Fig. 7 is missing at 13:50 and 14:20. Similarly, Fig. 8 shows a similar cross-section for the storm above Austria.

Comparing the position of highest tops with the cold ring and CWS shows (Figs. 6 and 7) that the CWS begins to evolve at the downwind side of the elevated dome, spreading downwind, above the stratiform part of the anvil. This is consistent with what was shown for the cold-U shaped storms (references above), and supports our suspicion that the two forms of storms are closely related. At the end of the life of the elevated dome, with its decay, the warm area spreads upwind, embedding the overshooting tops area. This might explain the spatial arrangement of the CWS and the high dome in Fig. 8, where the entire dome is already located inside the warm area.

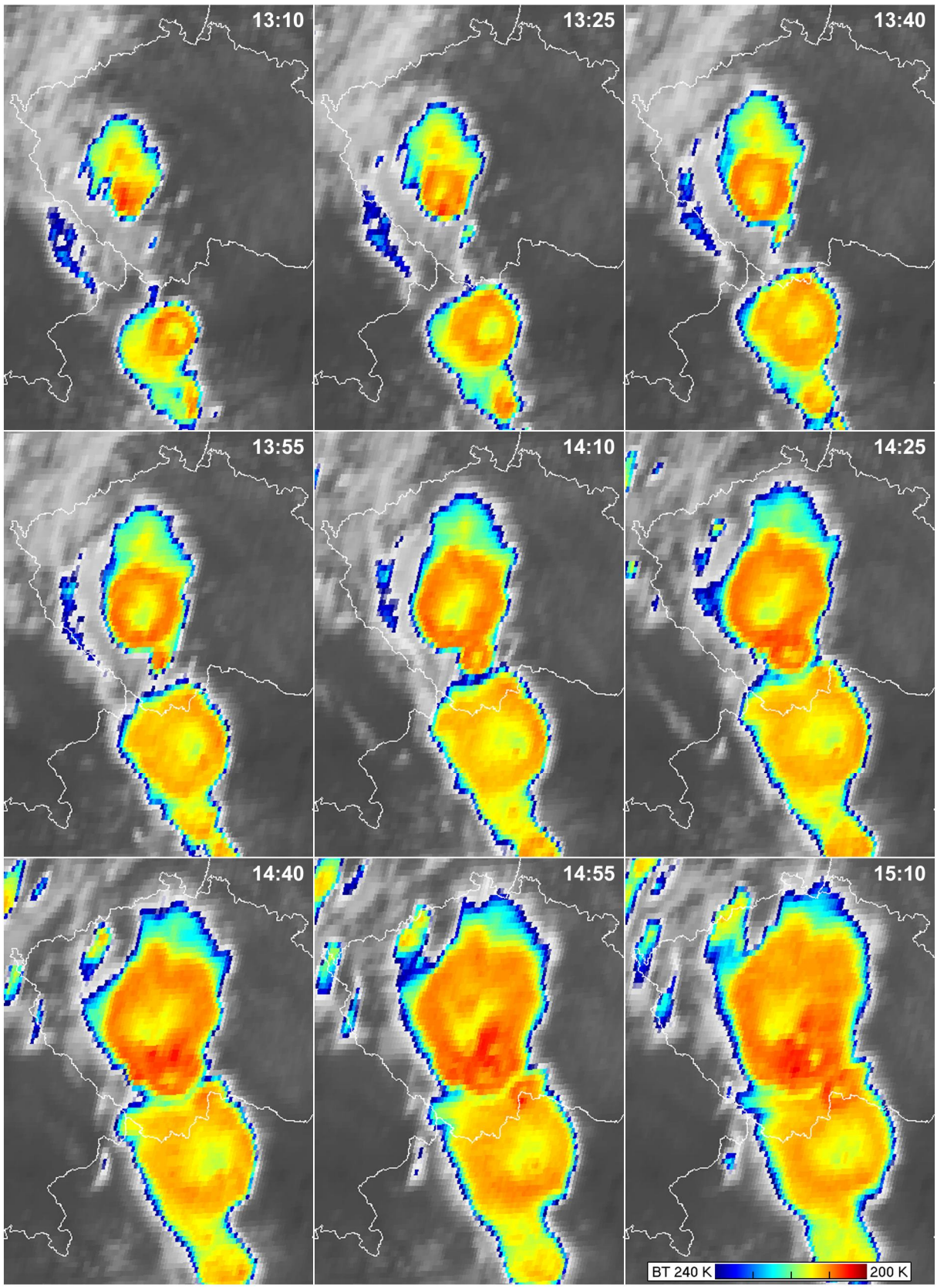

Figure 3: **Evolution of the cold-ring shaped storms of the 25 June 2006 (same as in the Fig.2), 13:00 - 15:00 UTC, Meteosat-8 (MSG-1), color-enhanced IR10.8 band, Czech Republic and Austria. Note: all the time stamps throughout this paper refer to the scanning time of the area by the Meteosat-8 satellite, while the time stamps of radar data refer to the header time of the radar measurement. For further comments on this please see the text of the paper.**

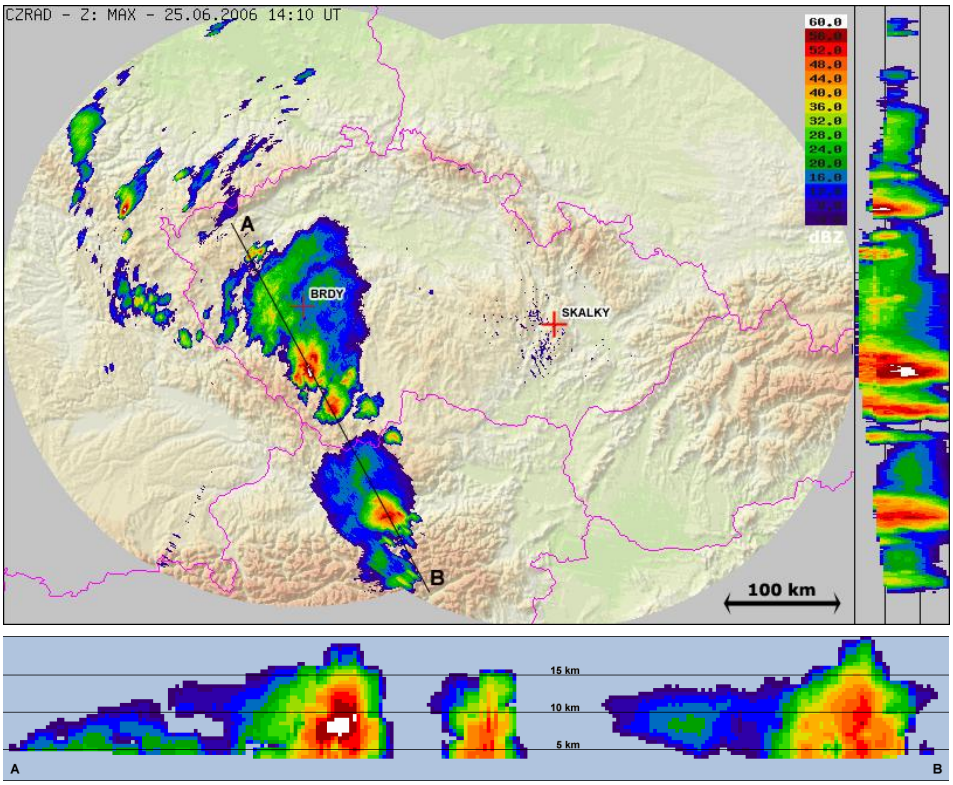

Figure 4: **Radar image (maximum reflectivity product, and side view) of the storms of 25 June 2006, 14:10 UTC (top), and corresponding cross-section along the line AB (bottom). While the operationally generated side projections range up to the 14 km level, the experimental cross-section shows the storm echo tops (lowest shown radar reflectivity being 4 dBZ) up to 20 km. The operational product is based on data from both CHMI radars (Brdy and Skalky, their position being indicated by red crosses), and the experimental cross-section is based on Skalky radar data only (at about 200 km from the storms).**

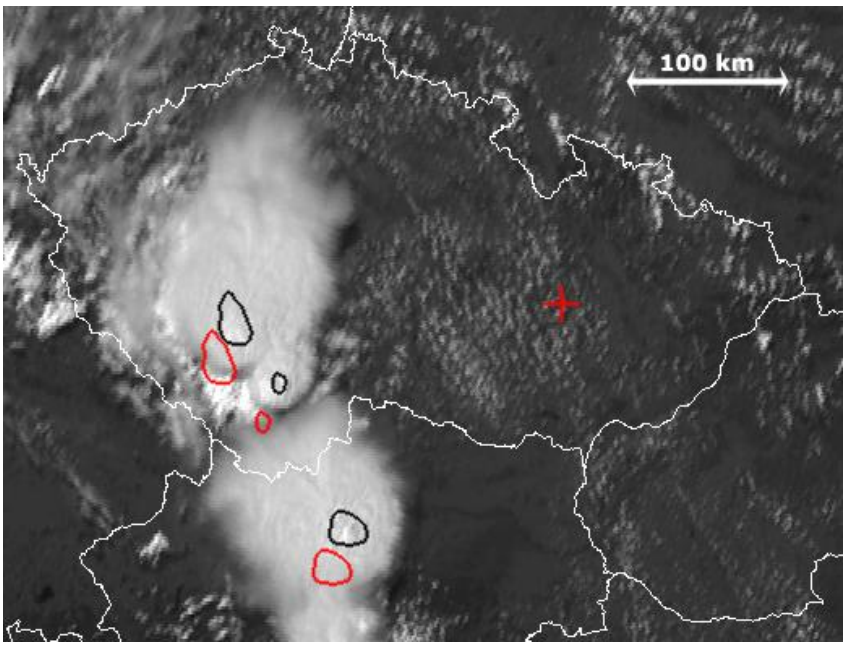

Figure 5: **Demonstration of the parallax effect when comparing satellite data (in this case geostationary satellite Meteosat-8, 25 June 2006, 14:10 UTC) with operational radar data. The red contours show the original positions of overshooting tops as observed by radar (determined by CAPPI 15.5 km level here), and the black contours after corresponding parallax shift applied to the radar CAPPI data (as if observed from the Meteosat-8 satellite). While the original (red) contours are apparently located partially outside the anvil edges, the parallax-shifted ones (black) match well with the position of the overshooting tops as observed by the satellite in this HRV image. The red cross shows the position of the Skalky radar, which was used for this study.**

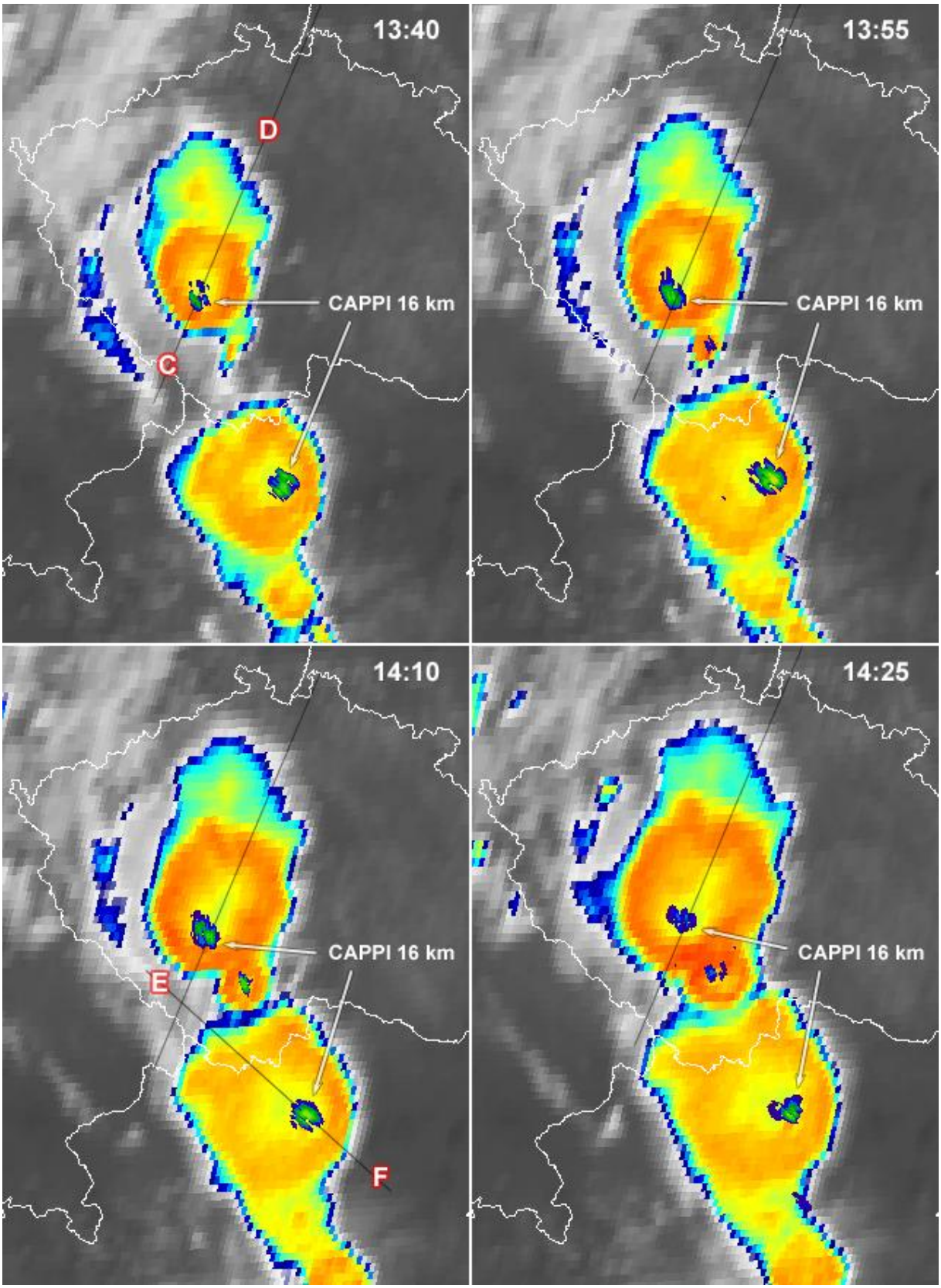

Figure 6: **Color-enhanced Meteosat-8 IR10.8 images (color scale the same as in Figures 1, 2 and 3), overlaid with radar CAPPI 16 km images, artificially shifted to the satellite projection (the radar reflectivity scale for these is in Figure 4). The black lines CD (all times) and EF(14:10 only) indicate the position of the cross-sections in Figures 7 and 8.**

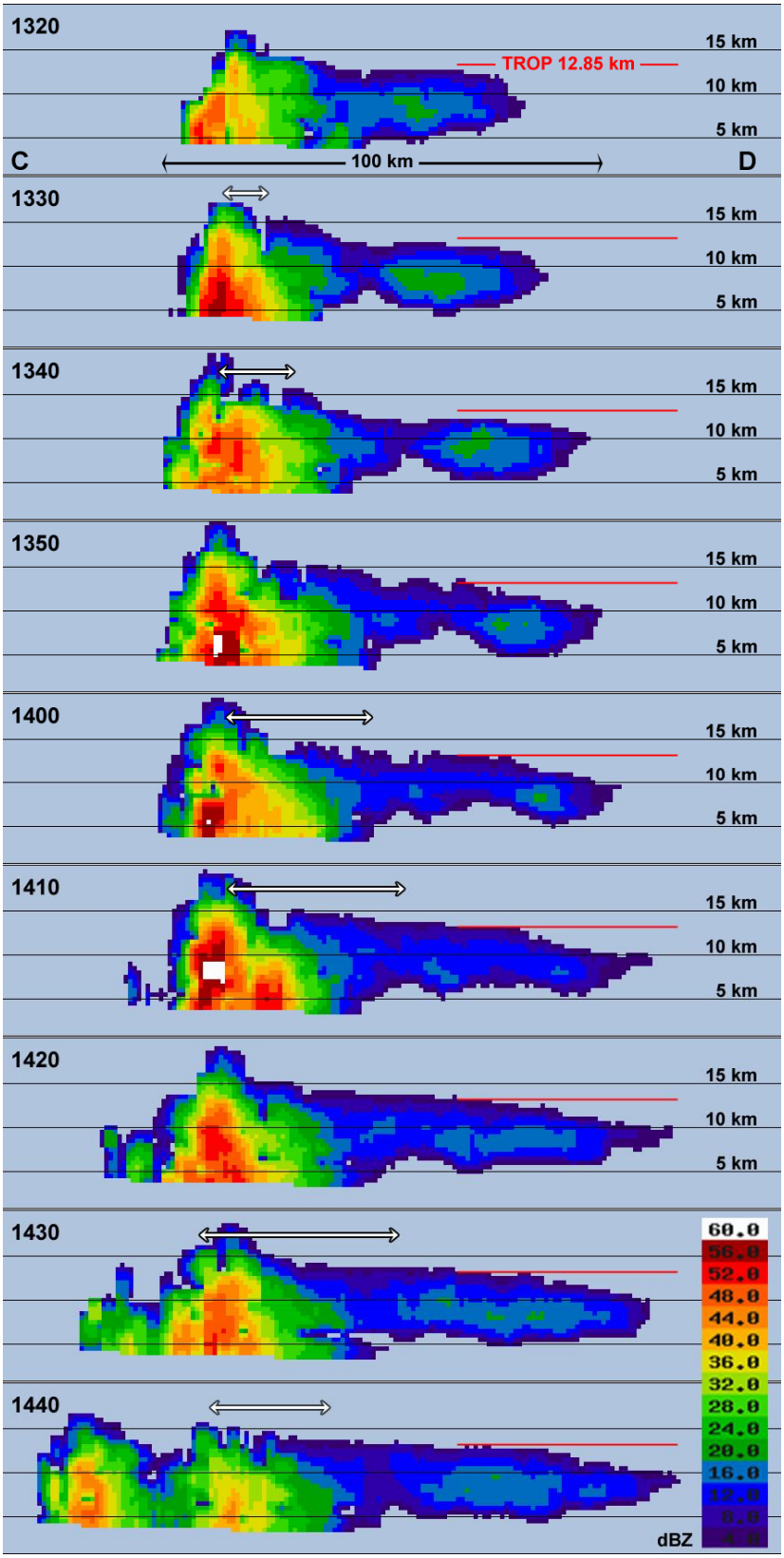

Figure 7: **Radar cross-section of the storm along the lines CD indicated in Figure 6, from 1320 to 1440 UTC. The red line indicates the tropopause height (from Prague 12 UTC sounding), and the double-arrow shows the position and extent of the individual CWS (where available from the MSG imagery) with respect to the radar data. For 13:20, 13:50 and 14:20 no CWS position was plotted here due to a timing discrepancy of the satellite and radar imagery; the CWS appeared first at the 13:25 satellite image.**

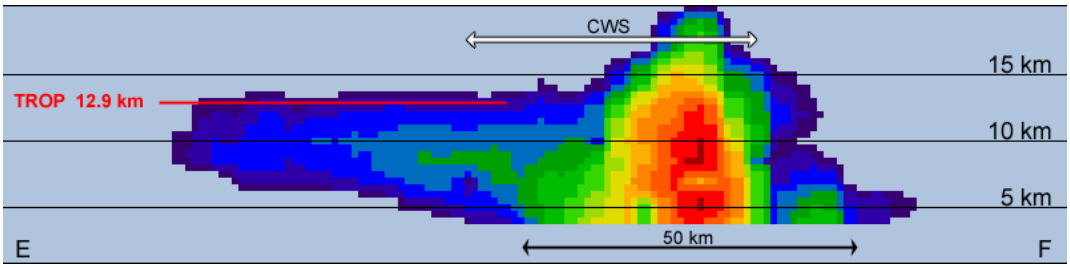

Figure 8: **Similar to Figure 7, but for the storm above Austria, at 14:10 UTC, along the line EF. The tropopause height in this case is from the Vienna sounding (ahead of the storms); another sounding in the area (Munich, already behind the storm system) placed the tropopause at 12.6 km. The radar reflectivity scale is the same as in Figure 7. For the discussion of the cross-section and its link to the CWS please see the text of the paper.**

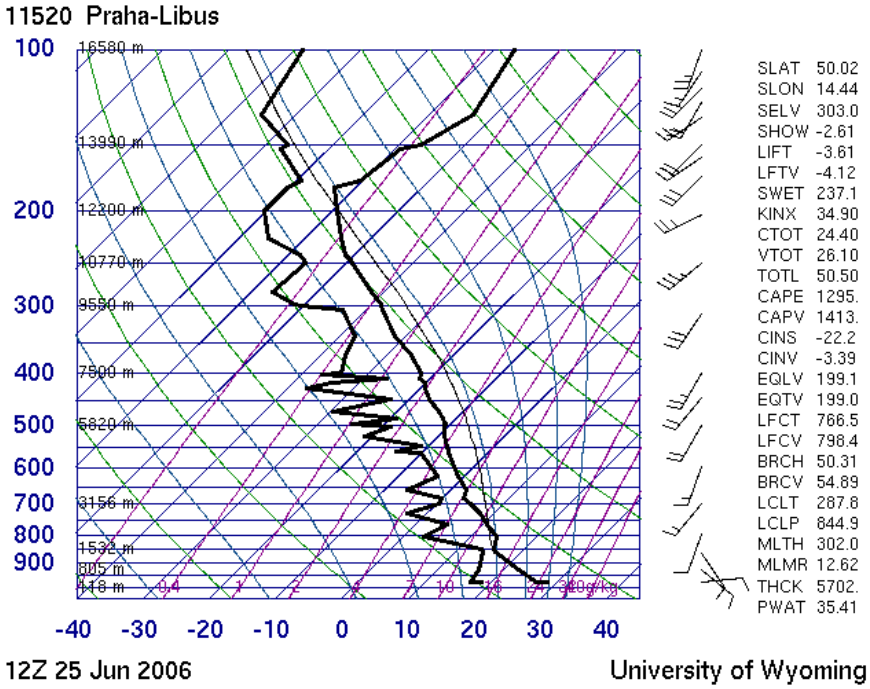

Figure 8: **Prague 25 June 2006 12 UTC sounding, documenting the strong thermal inversion above the tropopause, and the rather weak wind shear at the upper levels. The low levels exhibit some vertical wind shear, typical for supercell environments.**

Soundings from Prague (Fig. 9), obtained just before the storms' formation, document a strong thermal inversion above the tropopause, without which the cold-ring and CWS probably would have not formed (Schlesinger, 1988). The wind shear at cloud top levels is rather weak, which might be the crucial factor discriminating between the formations of cold-U and cold-ring shaped storms.

GENERAL CHARACTERISTICS OF COLD-RING SHAPED STORMS

In general, cold-ring shaped storms are not uncommon in Europe. Every year, they are observed on 10 – 20 days, at various regions over the continent, and of various magnitudes. It seems that their occurrence is supported by some specific airmass types – probably with a certain combination of weaker upper-level wind shear and a strong thermal inversion above the tropopause. However, most of the cold-ring shaped storms have much shorter lifetimes than the case documented above. Typically, the warm spot is attached downwind to a cold overshooting top, disappearing shortly after the decay of the overshoot. However, there are several cases of long-lived cold-ring/CWS couplets (of the order between 1 to 2 hours) documented over the last few years, all of these cases having produced severe weather (http://convection.satreponline.org/, or Image Gallery at http://www.eumetsat.int/). A problem is posed by the fact that there is no objective, quantitative definition of cold-ring shaped storms (in terms of temperature differences between the cold-ring

minimum and CWS maximum, size and duration of these). A typical CWS size is from several SEVIRI pixels, up to about 50 km, and the temperature difference between the cold ring minimum and CWS maximum is typically from several degrees up to about 10 – 12 K. However, since this temperature difference depends on the temperature minimum of the "parent" overshooting top, this characteristic has a somewhat lower significance. While the maximum BT difference during a storm's lifetime could be related to storm intensity, sampling that value may be difficult considering its rapid temporal fluctuations and the limited sampling intervals of current operational satellites. Also, it should be stressed here that in the case described above the highest tops (documented by radar observations) were not pronounced in the IR brightness temperature (BT) – these tops were at the same BT as the rest of the cold ring or even composed part of the CWS for the entire period of its presence. This was the main reason why these tops escaped their detection when applying the SAFNWC cloud top height algorithm (http://nwcsaf.inm.es/). Further comments on this can be found in Šťástka and Setvák (2008). Also, since the warm spots significantly increase the average brightness temperature of the entire storm's cloud top, their presence will lead to underestimation of the storm's potential for severe weather or heavy rainfall.

Besides Europe, several cold-ring shaped storms were also found above the continental United States, as well as above the Mediterranean region and the Arab Peninsula. No cold-ring shaped storms have been observed over tropical parts of Africa or South Africa (the area scrutinized ranged from 6° N to the south tip of Africa. No other geographical regions were checked in detail so far.

LINK BETWEEN COLD-RING AND COLD-U SHAPED STORMS

Since it appears that both types of storms are caused by a similar mechanism, the question stands what discriminates between these. It appears that the crucial factor may be the upper-level wind shear (storm-relative); this hypothesis is presently being investigated by authors of this paper (PKW and DTL). The link between the two types of storms seems to be strongly supported by a documented case of transition of a cold-ring shaped storm into a cold-U type (e.g. the storm shown in Fig. 1). Another factor for consideration is the possibility of a "plume masking mechanism" (Setvák et al, 2007), in which a warmer above-anvil plume (Levizzani and Setvák, 1996), also related to the upper-level wind shear, might "mask" part of the cold ring underneath, at the downwind side of the ring.

CONCLUSIONS AND OUTLOOK

The presented case seems to indicate that the formation mechanism for the cold-ring and CWS couplet is similar to the one responsible for the formation of cold-U shaped storms. This hypothesis will be further studied by means of numerical modeling. Since the radar cross-sections cannot exclude the presence of warm, above-anvil cirrus (the C-band radar is not capable of distinguishing it), we continue searching for a cold-ring shaped storm intersected by the A-Train satellites. If such a storm is found, the CloudSat and CALIPSO observations (combined with MODIS/Aqua and available geostationary satellite, either MSG or GOES) are likely to provide significant contribution to our understanding of these types of storms. Finally, a representative study (PhD thesis) of one of the authors (MR) will address representative number of similar cases within the range of CHMI radars, comparing satellite, radar and sounding observations, with respect to the cold-ring and cold-U shapes occurrence.

Since the warm spots (CWS) tend to form in the lee of significant overshooting tops, they may serve as one of the features indicating possible storm severity. In particular, long-lived cold-ring shaped storms should by treated carefully, given their high chance of producing severe weather. At the same time, they are likely to be underestimated by various cloud-top derived products (Šťástka and Setvák, 2008).

ACKNOWLEDGEMENTS

Major parts of this research were carried out under support of the Grant Agency of the Czech Republic, project no. 205/07/0905, and within frame of the ESSL and EUMETSAT Convection Working Group activities.

REFERENCES

Adler, R. F., Markus, M.J., and Fenn, D.D., (1985) Detection of severe Midwest thunderstorms using geosynchronous satellite data. Mon. Wea. Rev., **113**, pp 769-781

Adler, R. F., and R. A. Mack, R.A., (1986) Thunderstorm cloud top dynamics as inferred from satellite observations and a cloud top parcel model. J. Atmos. Sci., **43**, pp 1945-1960

Brunner, J.C., Ackerman, S.A., Bachmeier, A.S., and Rabin, R.M., (2007) A Quantitative Analysis of the Enhanced-V Feature in Relation to Severe Weather. Wea. Forecasting, **22**, pp 853-872

Dotzek, N., Rabin R.M., Carey, L.D., MacGorman, D.R., McCormick, T.L., Demetriades N.W., Murphy, M.J., Holle R.L., (2005) Lightning activity related to satellite and radar observations of a mesoscale convective system over Texas on 7-8 April 2002. Atmos. Research, **76**, pp 127-166

Fujita T.T., (1982) Principle of stereoscopic height computations and their applications to stratospheric cirrus over severe thunderstorms. J. Meteor. Soc. of Japan, **60**, pp 355-368

Heymsfield, G.M., Blackmer Jr., R.H., and Schotz, S., (1983a) Upper level structure of Oklahoma tornadic storms on 2 May 1979, Pt. 1 radar and satellite observations. J.Atmos.Sci., **40**, pp 1740-1755

Heymsfield, G. M., Szejwach, G., Schotz, S., and Blackmer Jr., R.H., (1983b) Upper level structure of Oklahoma tornadic storms on 2 May 1979, Pt. 2 Proposed explanation of “V” pattern and internal warm region in infrared observations. J. Atmos. Sci., **40**, pp 1756-1767

Heymsfield, G.M., Blackmer Jr., R.H., (1988) Satellite-observed characteristics of Midwest severe thunderstorm anvils. Monthly Weather Review, **116**, pp 2200-2224

Heymsfield, G. M., Fulton, R., and Spinhirne, J.D., (1991) Aircraft overflight measurements of Midwest severe storms: Implications on geosynchronous satelite interpretations. Monthly Weather Review, **119**, pp 436-456

Levizzani, V., and M. Setvák, M., (1996) Multispectral, high-resolution satellite observations of plumes on top of convective storms. J. Atmos. Sci., **53**, pp 361-369

Luderer, G., Trentmann, J., Hungershöfer, K., Herzog, M., Fromm, M., and Andreae, M.O., (2007) Small-scale mixing processes enhancing troposphere-to-stratosphere transport by pyro-cumulonimbus storms. Atmos. Chem. Phys., **7**, pp 5945–5957

McCann, D. W., (1983) The enhanced-V: A satellite observable severe storm signature. Mon. Wea. Rev., **111**, 887-894

Mills, P.B., and Astling, E.G., (1977) Detection of tropopause penetrations by intense convection with GOES enhanced infrared imagery. Preprints 10th Conf. Severe Local Storms, Omaha, Amer. Meteor. Soc., pp 61 - 64

Negri, A. J., (1982) Cloud-top structure of tornadic storms on 10 April 1979 from rapid scan and stereo satellite observations. Bull. Amer. Meteor. Soc., **63**, 1151-1159

Novák, P., (2007) The Czech Hydrometeorological Institute's severe storm nowcasting system. Atmos. Res., **83**, pp 450-457

Radová, M., and Seidl, J., (2008) Parallax applications when comparing radar and satellite data. The 2008 EUMETSAT Meteorological Satellite Conference. (this conference proceedings)

Schlesinger, R. E., (1984) Mature Thunderstorm Cloud-Top Structure and Dynamics:
A Three-Dimensional Numerical Simulation Study. J. Atmos. Sci., **41**, pp 1551–1570

Schlesinger, R. E., (1988) Effects of stratospheric lapse rate on thunderstorm cloud-top structure in a three-dimensional numerical simulation, Pt. 1, Some basic results of comparative experiments. Journal of Atmospheric Science, **45**, pp 1555-1570

Setvák, M., Rabin, R.M., and Wang, P.K., (2007) Contribution of the MODIS instrument to observations of deep convective storms and stratospheric moisture detection in GOES and MSG imagery. Atmos. Res., **83**, pp 505-518

Šťástka, J., Setvák, M., (2008) Cloud Top Temperature and Height product of the Nowcasting SAF applied to tropopause-penetrating cold-rinh shaped storms. The 2008 EUMETSAT Meteorological Satellite Conference. (this conference proceedings)

Wang, P.K., (2007) The thermodynamic structure atop a penetrating convective thunderstorm. Atmos. Res., **83**, pp 254-262